

## Baseline characterization of major Iberian vegetation types based on the NDVI dynamics

Domingo Alcaraz-Segura · Javier Cabello · José Paruelo

Received: 21 May 2007 / Accepted: 20 November 2008 / Published online: 13 December 2008  
© Springer Science+Business Media B.V. 2008

**Abstract** We present an approach to derive baseline conditions for the radiation intercepted by vegetation in the largest remaining patches of homogeneous vegetation of the Iberian Peninsula. These baseline conditions can serve as a reference to assess environmental changes. We also characterized the major vegetation types of the Peninsula in the functional space defined by the NDVI dynamics and analyzed the climatic controls of NDVI dynamics. We analysed the attributes of the NDVI seasonal dynamics: annual mean (NDVI-I), relative range (RREL), NDVI maximum and minimum values (MAX and MIN), months of MAX and MIN (MMAX and MMIN), and their inter-annual variabilities

(1982–1999). We selected as reference sites only homogeneous pixels occupied by natural vegetation. We described their relationship with climatic variables using regression models. NDVI-I and RREL captured most of the variability of the NDVI annual profile. Eurosiberian vegetation types were more productive, with winter minima and summer maxima. Mediterranean vegetation had summer minima and maxima distributed from autumn to spring. Inter-annual differences (higher in the Mediterranean) were low for NDVI-I and MAX and high for RREL and MIN. Precipitation was the main driver of NDVI-I for the Mediterranean pixels while temperature constrained it in the Eurosiberian ones. Seasonality (RREL) was associated with winter temperatures in Eurosiberian areas and with summer drought in Mediterranean ones. The Iberian vegetation types mainly differed in terms of total production and seasonality. Such differences were related to mean and inter-annual variation in precipitation and temperature associated with the Eurosiberian and Mediterranean climate zones. The NDVI dynamics allowed us to identify a functional signature for each vegetation type which captures differences that go beyond their range of climatic factors. Our baseline descriptions, based on a common approach to characterize vegetation functioning, are proposed as reference situations to evaluate the impact of environmental changes on the remaining large patches of single major natural and seminatural vegetation types.

---

D. Alcaraz-Segura (✉)  
Department of Environmental Sciences, University of Virginia, Clark Hall, 291, McCormick Road, Charlottesville, VA 22904-4123, USA  
e-mail: dalcaraz@ual.es

D. Alcaraz-Segura · J. Cabello  
Departamento de Biología Vegetal y Ecología,  
Universidad de Almería, La Cañada de San Urbano,  
04120 Almería, Spain

D. Alcaraz-Segura · J. Paruelo  
Laboratorio de Análisis Regional y Teledetección,  
Instituto de Investigaciones Fisiológicas y Ecológicas Vinculadas a la Agricultura (IFEVA), Universidad de Buenos Aires-Consejo Nacional de Investigaciones Científicas y Tecnológicas (CONICET), Av. San Martín 4453, 1417 Buenos Aires, Argentina

**Keywords** AVHRR/NOAA · Ecosystem functioning · Iberian Peninsula · Normalized Difference Vegetation Index (NDVI) · Regional analysis · Remote sensing

## Introduction

The effects of global environmental changes are particularly noticeable at the ecosystem level and at regional scales (Vitousek et al. 1997; Wolters et al. 2000). However, characterizations of the baseline conditions of ecosystems on extensive regions are relatively scarce in comparison with reference descriptions at the species, population, and community levels (Fazey et al. 2005). In addition, vegetation descriptions have been traditionally based just on structural features (such as physiognomy, dominant species, or floristic composition) derived from a few plot observations (e.g., Mueller Dombois and Ellenberg 1974; Stephenson 1990) but omitting functional attributes at the ecosystem level. Ecosystem functioning (i.e., the exchange of energy and matter between the ecosystem and the atmosphere Valentini et al. 1999) clearly complements traditional studies, since it shows a shorter response to environmental changes than vegetation structure (Milchunas and Lauenroth 1995; Wiegand et al. 2004). Monitoring ecosystems functioning by assessing ecological processes such as carbon gains or evapotranspiration allows a direct measurement of ecosystem services (Daily 1997). In addition, functional attributes of ecosystems can be easily and frequently monitored through remote sensing (Puelo et al. 2001), which is particularly useful for monitoring vegetation dynamics and ecosystem responses to environmental changes.

Currently, remote sensing provides adequate methods to produce a spatially continuous characterization of vegetation functioning at regional scale (e.g., Xiao and Moody 2004; Alcaraz-Segura et al. 2006). Both theoretical and empirical analyses provide support to the relationship between spectral indices derived from satellite images and functional attributes such as primary production (Pettorelli et al. 2005), the most integrative and essential indicator of ecosystem functioning (McNaughton et al. 1989; Virginia and Wall 2001). The most widely used of such indices is the Normalized Difference Vegetation Index (NDVI),

which is calculated from the reflectance in the red and near infrared wavelengths ( $[\text{NIR} - \text{R}]/[\text{NIR} + \text{R}]$ ; Tucker and Sellers 1986). The NDVI can be used to estimate the fraction of Absorbed Photosynthetically Active Radiation by vegetation (fAPAR) (Myneni and Williams 1994), the main control of primary production (Monteith 1972). The NDVI temporal dynamics provides critical information about the land-surface phenology and seasonality of vegetation, which is of great importance to determine the different strategies of carbon gains (Mooney et al. 1977; Orshan 1989).

The characterization of the baseline conditions of functional attributes of vegetation for the assessment of global change impacts has been frequently accomplished in protected areas (e.g., Garbulsky and Puelo 2004; Alcaraz-Segura et al. 2008a). However, restricting studies to protected areas may not provide enough extent and replications for the whole spectrum of vegetation types in a region. Moreover, the abrupt change of the disturbance regimes often associated with protection may initiate an ecological succession that obscures the signal of global drivers of change, such as changes in climate or in the atmospheric composition (Alcaraz-Segura et al. 2008b). Both constraints can be solved by extending studies to natural areas not subjected to land-use change, i.e., areas dominated by native vegetation subjected to a minimum human intervention and whose dynamics is mainly controlled by natural factors such as precipitation, temperature, and soils.

In this article, we present an approach to derive baseline conditions for the radiation intercepted by vegetation in the largest remaining patches of homogeneous vegetation of the Iberian Peninsula. These baseline conditions can serve as a reference to assess environmental changes. We also characterize the major vegetation types of the Peninsula in the functional space defined by the NDVI dynamics. Finally, we explore the climatic controls of the radiation interception.

## Methods

### Study area

The Iberian Peninsula (Fig. 1) is one of the most diverse areas of Europe and a region particularly

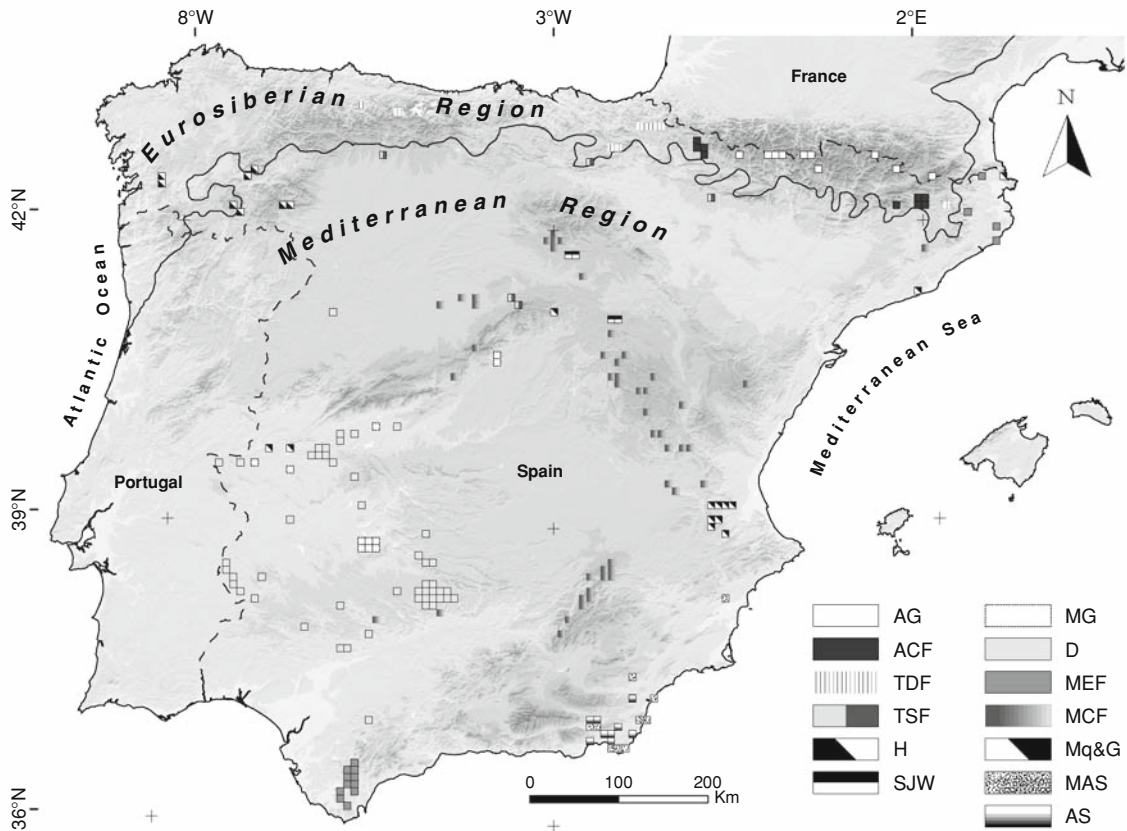


**Fig. 1** Spatial distribution of the 200 NOAA/AVHRR  $8 \times 8$  km pixels with more than 70% of their surface corresponding to one of the 12 Iberian major vegetation types studied. See “Study Area” subsection for vegetation type abbreviations

sensitive to biodiversity losses due to climate and land-use changes (Valladares et al. 2004). Natural areas cover large part of it despite having been intensively used for millennia. Two biogeographic regions, the Eurosiberian and the Mediterranean, are present in the Peninsula (Rivas-Martínez 1987; Fig. 1). The Eurosiberian region is characterized by a humid climate of oceanic influence, with fairly cold winters and water availability throughout the year, making vegetation phenology tightly linked to temperature seasonality and photoperiod (Lieth 1974; Rathcke and Lacey 1985). Five major vegetation types were studied in this region: Alpine natural and seminatural grasslands (AG), Alpine needleleaf coniferous forests (ACF), Temperate broadleaf deciduous forests (TDF), Temperate semideciduous forests (TSF), and Heathlands (H). The Mediterranean

region is characterized by a dry climate with mild, rainy winters and hot, dry summers. The presence of low winter temperatures and summer droughts (the main stress for Mediterranean vegetation; Blondel and Aronson 1999) generates two temporal “windows” for plant growth: spring and autumn (Mitrakos 1980). Eight vegetation types were studied in the Mediterranean region: Spanish Juniper woodlands (SJW), Mediterranean natural and seminatural grasslands (MG), Dehesas (D), Mediterranean evergreen sclerophyllous forests (MEF), Mediterranean needleleaf coniferous forests (MCF), Maquis and garrigues (Mq&G), Mediterranean semiarid scrublands (MAS), and Alpha-steppes (AS). Dehesas are savanna-like systems comprising an open overstorey of evergreen *Quercus* trees over an understorey of herbaceous annual and perennial species used by livestock.

## Selection of study sites for each vegetation type

Identifying large areas of natural vegetation in a region with an extensive history of human interventions and a very patchy distribution of ecosystems represents a difficult task. Therefore, we considered as “natural” only those areas with low human influence (i.e., not cropped or urbanized) and whose dynamics is mainly controlled by natural factors (such as climate, soils, or landscape structure) and disturbances. To simplify the high heterogeneity of the Iberian vegetation, we worked at the level of the 12 major vegetation types named above, i.e., extensive areas of natural and seminatural vegetation types, homogeneous in terms of physiognomy (relative abundance and dominance of plant functional types). Although they are not strictly natural, we included Dehesas and Mediterranean coniferous forests in the analysis because of their high extent and importance for nature conservation in Spain (Costa et al. 2005), and because they are relatively stable (Stevenson and Harrison 1992).

To select the study sites for the Iberian vegetation types, we used 1027 digital maps of the Spanish Forest Map (MFE200—Mapa Forestal de España 1:200,000; Ruíz de la Torre 1999). First, all polygons were reclassified to one of the former 12 major vegetation types considering the information in the MFE200 and the potential-vegetation map of Spain (generalized by us from Rivas-Martínez 1987; as specified in Alcaraz-Segura et al. 2006). Only sites larger than  $8 \times 8$  km (pixel size of the imagery used in the study; see below) and dominated (more than 70%) by the same major vegetation type were pre-selected. Then, to validate this pre-selection, we used the 1990 CORINE Land Cover database (EEA 2000) to discard those pre-selected sites of the MFE200 with lower than 70% of the equivalent land-cover in the CORINE database. The MFE200 was developed from aerial photographs from 1985, while CORINE used satellite images from 1986 to 1996. We also checked that these pixels did not contain a significant surface of changes from 1990 to 2000 in the CORINE land cover change map (EEA 2007). We assumed that sites corresponding to a particular vegetation type near the beginning and end of the study period remained representative of the same vegetation type during the whole period. Besides, although land-cover could be altered by human activities, these

changes are more subtle and slow in squares of  $64 \text{ km}^2$ . The final number of  $8 \times 8$  km sites was 200 (Fig. 1).

## Analysis of the NDVI imagery

We based our analysis on the 10-day NDVI composites provided by the 8-km PAL (Pathfinder AVHRR—Advanced Very High Resolution Radiometer—Land) dataset, available for the 1981–1999 period. This dataset has been corrected for atmospheric and orbital distortions (but not for volcanic aerosols; details in James and Kalluri 1994) and is used in a very large number of research studies (Hicke et al. 2002; Lobell et al. 2002; Nemani et al. 2003; Paruelo et al. 2004; Julien et al. 2006; Sobrino et al. 2006; de Beurs and Henebry 2007; Baldi et al. 2008; Sarkar et al. 2008). The scenes have an approximate spatial resolution of  $8 \times 8$  km and cover the whole globe. We used the portion of the images located between  $35^\circ \text{ N}$  and  $45^\circ \text{ N}$  in latitude and  $3.5^\circ \text{ E}$  and  $10.2^\circ \text{ W}$  in longitude in correspondence with the Iberian Peninsula. The long period considered includes both extremely dry and wet periods in the Peninsula (de Castro et al. 2005). Though new databases have been generated from the original AVHRR data (i.e., Global Inventory Modeling and Mapping Studies (GIMMS) dataset), we decided to use the PAL data (extending up to 1999) because evaluations based on the detection of ecosystem changes suggest a better performance of PAL than GIMMS, as PAL detects trends that match the expected shifts (Baldi et al. 2008). In addition, as we worked with individual PAL pixels, we were able to remove any remaining noise in the dataset associated with cloud contamination and spurious high values (e.g., data transmission errors). The 10-day composites were layer-stacked to create a 36-band image for each year. Years 1981 and 1994 were discarded due to bad quality of the data. Those problems not removed by the original processing of the PAL-database, associated with cloud contamination, incomplete atmospheric correction, off-nadir views or angular effects, and sensor degradation, were minimized by selecting the maximum NDVI value for each pixel from the three 10-day composites of each month (as proposed by Holben 1986). In order to further minimize noise and spurious values, negative values were replaced by zeros, and extreme

values were eliminated manually. The monthly NDVI images were examined visually to check for further possible erroneous pixels to be removed manually. In coastal pixels, the influence of the ocean signal was minimized by both the spatial maximum NDVI value composite of the PAL dataset and by the temporal maximum NDVI value composite applied every 10 days in the PAL dataset and every month in this study (Holben 1986). In any case, we visually checked the NDVI profiles to check that they were not affected by the ocean signal. Finally, we calculated the monthly NDVI values of the period as the mean of the 18 years considered. Averaging the monthly NDVI values of an 18-year period minimized the effect of the atmospheric scattering caused by the eruption of Mount Pinatubo in 1991. The final range of values varied between 0.1 and 0.75.

In order to describe the patterns of the interception of radiation by vegetation, the following variables were derived from the mean seasonal NDVI profiles (Fig. 2): annual mean (NDVI-I), annual relative range (RREL; difference between maximum and minimum NDVI divided by annual mean), maximum and minimum NDVI values (MAX and MIN), and months of the maximum and minimum values of NDVI (MMAX and MMIN). These variables describe in a straightforward way the height and shape of the NDVI seasonal profile, and capture important features of ecosystem functioning for temperate ecosystems (Xiao and Moody 2004; Pettorelli et al. 2005). NDVI-I can be used to estimate fAPAR (Sellers et al. 1996) and thus net primary production (Tucker

et al. 1985; Sellers et al. 1992; Paruelo et al. 1997). RREL (annual amplitude normalized by the NDVI annual mean) provides an indicator of the seasonality of the photosynthetic activity, i.e., a descriptor of how different carbon uptake is between the growing and non-growing seasons (Paruelo and Lauenroth 1995). RREL keeps the biological meaning of the absolute range or amplitude but standardized by the mean NDVI in an equivalent way as the coefficient of variation (standard deviation divided by the sample mean) does (Alcaraz-Segura et al. 2006). MMAX and MMIN provide an additional description of vegetation phenology, indicating the intra-annual distribution of the periods with maximum and minimum photosynthetic activity (Lloyd 1990; Hoare and Frost 2004).

We analyzed and summarized the structure of the whole NDVI dataset by performing a principal component analysis (PCA). The input data for this analysis consisted of a matrix of 12 variables (the mean NDVI value of each month) and, as cases, the 200 pixels classified according to their major vegetation type. Then, we performed an ordination of the Iberian vegetation types by means of the two principal axes that summed up the variation in the NDVI seasonal profiles. We evaluated the relationship between the functional traits defined by the NDVI seasonal profiles and the first two axes of the PCA. We also used the same matrix to compare the NDVI seasonal profiles among vegetation types by performing a discriminant analysis (DA). The discriminant analysis located the centroids of each group in the space defined by the 12 months NDVI values and allowed us to compare the NDVI mean seasonal profile among vegetation types. Additionally, we performed ANOVA and post hoc comparisons following the Tukey's statistic for comparing the mean values of each NDVI-derived attribute among vegetation types. We also analyzed the inter-annual variability of these attributes by means of their coefficient of variation (the standard deviation in the case of MMAX and MMIN because they are qualitative data and do not have to be normalized). Finally, we explored the climatic controls of the radiation interception by assessing logarithmic and stepwise multiple linear regressions between the functional traits (only for NDVI-I and RREL, the two main descriptors of the NDVI seasonal curve in the Iberian Peninsula as observed here and in Alcaraz-Segura et al. 2006) and the following climatic variables: mean

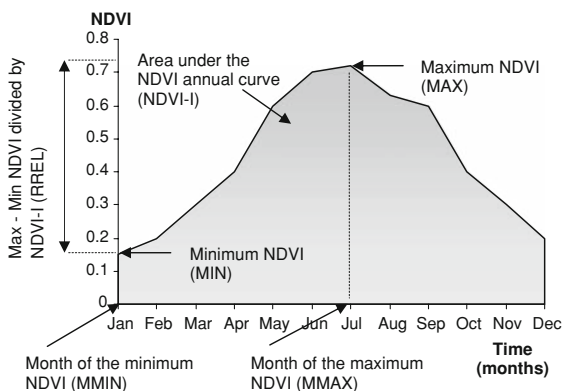


**Fig. 2** The six Normalized Difference Vegetation Index (NDVI) attributes employed in the functional characterization of the Iberian vegetation types (NDVI-I, RREL, MAX, MIN, MMAX, and MMIN)

annual precipitation (MAP, snow included), mean annual temperature (MAT), mean value of the maximum temperatures of the warmest month (TMAX) and mean value of the minimum temperatures of the coldest month (TMIN) (obtained from Sánchez-Palomares et al. 1999; Table 1).

## Results

### Ordination of the Iberian vegetation types by means of their NDVI seasonal dynamics

The first principal component (PCA-1) explained 73% of the spatial variability in the NDVI seasonal profile of the Iberian vegetation types (Table 2). PCA-1 was strongly related ( $r = 0.996$ ,  $n = 200$ ,  $P < 0.001$ ) to NDVI-I, a descriptor of productivity. The absolute value of the PCA-2, which accounted for 24% of the explained variance, was significantly associated with RREL ( $r = 0.752$ ,  $n = 200$ ,  $P < 0.001$ ) and can be interpreted, then, as a descriptor of seasonality. Three different relationships were found between PCA axes

1 and 2 (Fig. 3). All the Eurosiberian pixels had positive scores in the PCA-2 (highly seasonal) and showed a negative relationship between PCA-1 and PCA-2 ( $\text{PCA-2} = 1.863 - 0.869 \text{ PCA-1}$ ,  $r = 0.823$ ,  $n = 41$ ,  $P < 0.001$ ). Mediterranean grasslands and Dehesas displayed a different pattern with negative scores for PCA-2 and a slight, positive relationship between axes ( $\text{PCA-2} = -1.051 + 0.301 \cdot \text{PCA-1}$ ,  $r = 0.671$ ,  $n = 60$ ,  $P < 0.001$ ). Finally, the rest of the Mediterranean vegetation types showed no relationship between the PCA axes ( $r = 0.197$ ,  $n = 99$ ,  $P > 0.05$ ).

Alpha-steppes and Mediterranean semiarid scrubs were the least productive vegetation types and formed an isolated group in the negative extreme of PCA-1 (Fig. 3). Mediterranean coniferous forests were the most heterogeneous group, covering the highest range along PCA-1. Mediterranean sclerophyllous forests presented the highest values of productivity (PCA-1 or NDVI-I) and the lowest seasonalities (both in PCA-2 and RREL). Alpine grasslands showed the highest scores in PCA-2 and formed a heterogeneous but isolated group. Temperate deciduous forests also

**Table 1** Environmental characterization of the pixels analyzed for the Iberian natural and seminatural major vegetation types (Veg.T.)

Veg.T.	#	Altitude <sup>a</sup> (m)	MAP <sup>a</sup> (mm)	MAT <sup>a</sup> (°C)	TMAX <sup>a</sup> (°C)	TMIN <sup>a</sup> (°C)	Conspicuous species
AG	10	2261 ± 139	1449 ± 220	4 ± 1	14 ± 2	-6 ± 1	<i>Festuca eskia</i> , <i>F. indigesta</i>
ACF	9	1062 ± 130	1121 ± 280	10 ± 1	25 ± 1	-2 ± 1	<i>Pinus uncinata</i> , <i>P. sylvestris</i> , <i>Abies alba</i>
TDF	9	885 ± 156	1583 ± 423	10 ± 1	23 ± 1	-1 ± 1	<i>Fagus sylvatica</i> , <i>Quercus robur</i> , <i>Q. petraea</i> , <i>Alnus glutinosa</i>
TSF	5	975 ± 226	753 ± 117	10 ± 1	27 ± 1	-2 ± 1	<i>Quercus pyrenaica</i> , <i>Q. faginea</i>
H	8	1112 ± 356	1595 ± 195	9 ± 2	23 ± 2	-1 ± 2	<i>Erica</i> spp., <i>Calluna</i> spp., <i>Ulex europaeus</i>
SJW	4	1185 ± 56	613 ± 76	10 ± 0	27 ± 0	-2 ± 1	<i>Juniperus thurifera</i>
MG	11	494 ± 225	599 ± 113	15 ± 2	34 ± 2	2 ± 1	<i>Festuca scariosa</i> , <i>Helictotrichon filifolium</i> , <i>Brachypodium retusum</i> , <i>Bromus</i> spp.
D	49	478 ± 175	634 ± 85	16 ± 1	35 ± 1	3 ± 1	<i>Quercus suber</i> , <i>Q. rotundifolia</i>
MEF	15	339 ± 127	1059 ± 177	16 ± 1	29 ± 1	5 ± 2	<i>Quercus suber</i> , <i>Q. ilex</i> , <i>Q. rotundifolia</i>
MCF	48	1111 ± 295	688 ± 162	11 ± 2	29 ± 3	-1 ± 2	<i>Pinus pinaster</i> , <i>P. sylvestris</i> , <i>P. nigra</i>
Mq&G	13	568 ± 291	561 ± 159	14 ± 2	31 ± 3	2 ± 2	<i>Pistacia lentiscus</i> , <i>Quercus coccifera</i> , <i>Olea sylvestris</i> , <i>Cistus</i> spp., <i>Rosmarinus officinalis</i>
MAS	10	215 ± 237	272 ± 53	17 ± 1	32 ± 1	6 ± 2	<i>Anthyllis cytisoides</i> , <i>A. terniflora</i> , <i>Periploca laevigata</i> , <i>Genista retamoides</i>
AS	9	386 ± 184	295 ± 30	17 ± 1	31 ± 1	6 ± 1	<i>Stipa tenacissima</i>

See "Study Area" subsection for vegetation type abbreviations

MAP mean annual precipitation; MAT mean annual temperature; TMAX maximum temperature; TMIN minimum temperature

# Number of pixels

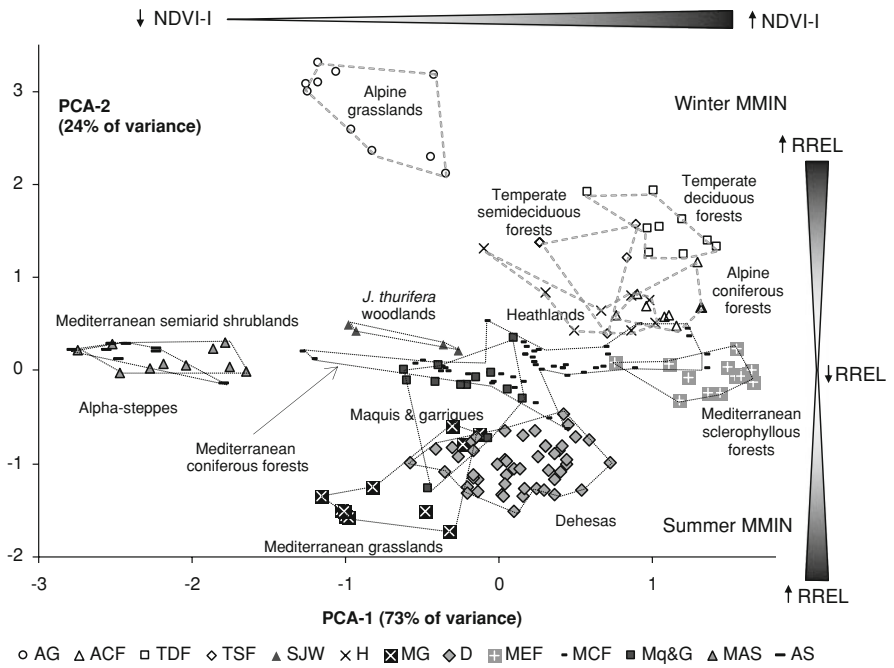
<sup>a</sup> Mean value ± spatial standard deviation

**Table 2** Eigenvectors and cumulative variance explained by the first two components of a principal component analysis (PCA) performed on the mean monthly NDVI values for the period 1982–1999 in the Iberian vegetation types

PCA axis	% <sup>a</sup>	Scores											
		Jan	Feb	Mar	Apr	May	Jun	Jul	Aug	Sep	Oct	Nov	Dec
1	73	0.845	0.801	0.810	0.854	0.965	0.857	0.779	0.784	0.802	0.915	0.975	0.878
2	97	-0.509	-0.586	-0.564	-0.478	0.001	0.503	0.621	0.615	0.591	0.382	-0.088	-0.425

<sup>a</sup> Cumulated variance

**Fig. 3** Functional space of the Iberian major vegetation types in terms of the first two axes of the Principal Component Analysis (PCA) carried out with the 12 NDVI monthly values. NDVI integer (NDVI-I) increases with PCA-1 ( $r = 0.996$ ). Annual relative range (RREL) increases toward the extremes of PCA-2 ( $r = 0.752$ ). Three different relationships between PCA-1 and PCA-2 can be observed: negative, positive, and none. Dashed lines correspond to the Eurosiberian vegetation types and continuous lines to the Mediterranean ones. See “Study Area” subsection for vegetation type abbreviations



displayed high positive values for PCA-2 but formed a more homogeneous group. Temperate semideciduous and Alpine coniferous forests as well as Heathlands showed some overlap in the plane of the first two PCA axes. In the opposite negative extreme of the PCA-2, Mediterranean grasslands and Dehesas had similar values of seasonality but differed in productivity.

Differences in the seasonal dynamics of the NDVI among Iberian vegetation types

The discriminant analysis showed significant differences in the seasonal profiles of NDVI among the Iberian vegetation types (Fig. 4, Appendix). In general, Alpine grasslands, Temperate deciduous forests, and Mediterranean grasslands were the most distinct vegetation types. Alpine grasslands and both

Mediterranean grasslands and Dehesas showed the highest differences. The most similar classes were (1) Alpha-steppes and Mediterranean semiarid scrubs (but quite distinctive from the rest), (2) Mediterranean coniferous forests and Maquis and garrigues, (3) Temperate semideciduous forests and both Heathlands and Spanish Juniper woodlands, and (4) Mediterranean grasslands and Dehesas (Fig. 4, Appendix). The largest differences among vegetation types occurred in summer (Fig. 4). In general, NDVI-I was higher for the Eurosiberian vegetation types (with the exception of Alpine grasslands), even though Mediterranean sclerophyllous forests showed the highest NDVI-I (Fig. 5a). The lowest values corresponded to Alpha-steppes and Mediterranean semiarid scrubs. Seasonality (RREL) was higher in grasslands systems (Alpine grasslands, Mediterranean

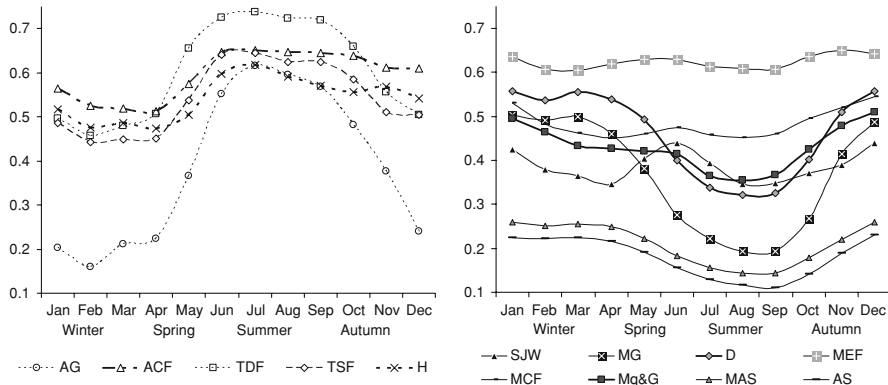
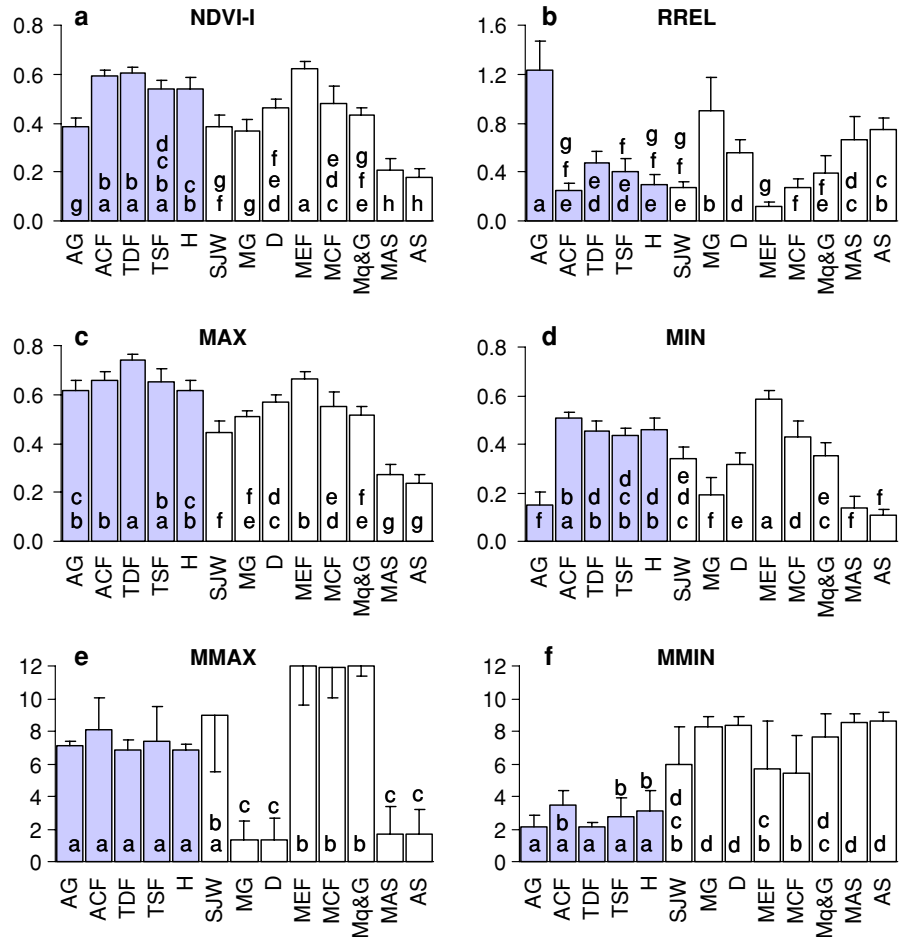


**Fig. 4** Mean seasonal profile of the NDVI in the Iberian vegetation types. Each *point* represents the mean value for all pixels with the same major vegetation type and for the 18 years analyzed. *Dashed lines* correspond to the Euro Siberian

vegetation types and *continuous lines* to the Mediterranean ones. See “Study Area” subsection for vegetation type abbreviations

**Fig. 5** Functional characterization of the Iberian vegetation types in terms of the mean values of the NDVI annual mean (a), annual relative range (b), maximum and minimum values of NDVI in the year (c, d), and the months of maximum and minimum NDVI values (e, f). *Vertical lines* on top of the bars represent the spatial standard deviation of each NDVI-derived attribute. *Different letters* indicate significant differences ( $P < 0.01$ ; Tukey’s test). *Gray bars* correspond to the Euro Siberian vegetation types and *white bars* to the Mediterranean ones. See “Study Area” subsection for vegetation type abbreviations



grasslands, and Alpha-steppes), while evergreen vegetation showed the lowest differences throughout the year (e.g., Mediterranean sclerophyllous forests)

(Fig. 5b). The maximum values of NDVI (MAX) showed a similar pattern than NDVI-I. MAX was higher in the Euro Siberian vegetation types and



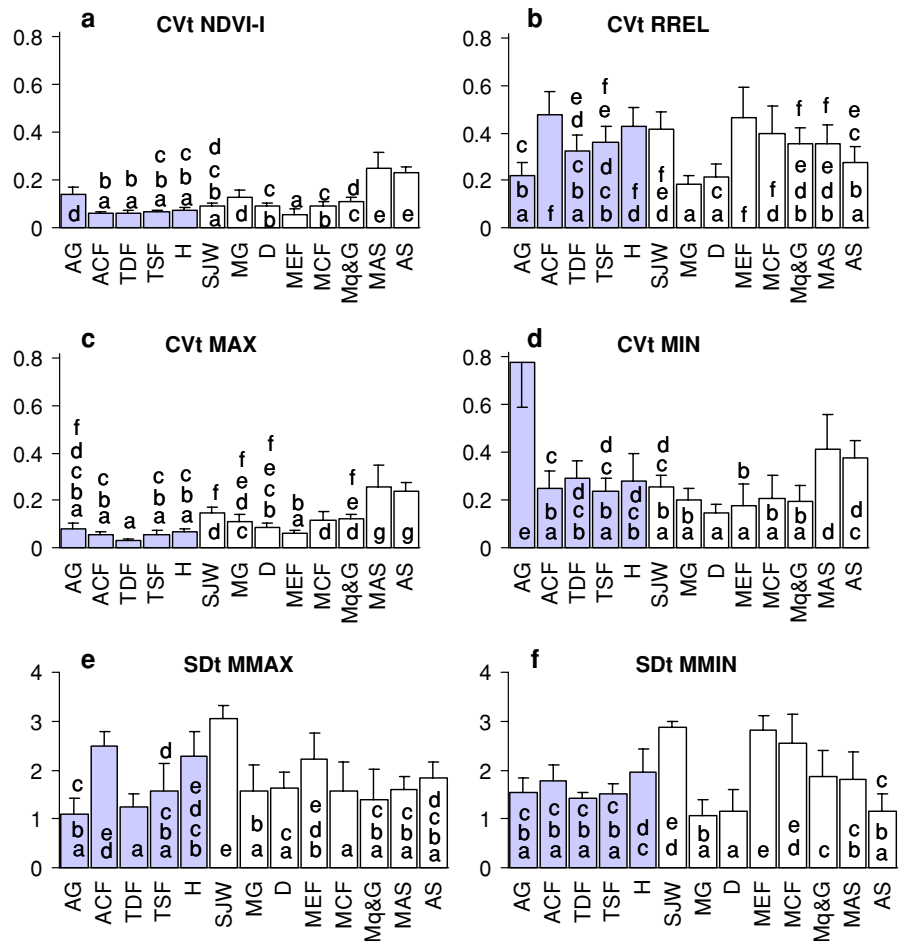
showed the lowest values in semiarid systems (Mediterranean semiarid scrubs and Alpha-steppes) (Fig. 5c). The lowest NDVI minima (MIN) occurred in the grasslands and arid systems (Alpine grasslands, Mediterranean grasslands, Alpha-steppes, and Mediterranean semiarid scrubs), while Mediterranean sclerophyllous forests had the highest MIN (just 10% lower than MAX) (Fig. 5d). All Eurosiberian vegetation types had their maximum NDVI in summer, while the month of the maximum (MMAX) for the Mediterranean vegetation types varied from autumn to spring (Fig. 5e). Nevertheless, there were some Mediterranean pixels with summer maxima (Mediterranean sclerophyllous forests, Mediterranean coniferous forests, and Spanish Juniper woodlands). The minima occurred in winter in the Eurosiberian vegetation types (Fig. 5f). In the Mediterranean vegetation types, most pixels had their minimum (MMIN) in summer, although some pixels showed

winter minima (Mediterranean sclerophyllous forests, Mediterranean coniferous forests, and Spanish Juniper woodlands).

Inter-annual variability of the NDVI dynamics in the Iberian vegetation types

In general, inter-annual variabilities (coefficients of variation) were low for NDVI-I and MAX, and high for RREL and MIN (Fig. 6). Grasslands and arid vegetation types (Alpine grasslands, Mediterranean grasslands, Alpha-steppes, and Mediterranean semiarid scrubs) showed the highest inter-annual variability for NDVI-I (Fig. 6a). The inter-annual variability of RREL was lower for Alpine and Mediterranean grasslands and Dehesas, while the highest values occurred in Mediterranean sclerophyllous and Alpine coniferous forests (Fig. 6b). Inter-annual differences of MAX (Fig. 6c) were significantly higher for the

**Fig. 6** Differences in inter-annual variability of the Iberian vegetation types from 1982 to 1999 measured through the temporal Coefficient of Variation (CVt) of the NDVI annual mean (a), annual relative range (b) and maximum and minimum values of NDVI in the year (c, d), and temporal Standard Deviation (SDt) of the months of maximum and minimum NDVI values (e, f). Vertical lines on top of the bars represent the spatial standard deviation of each NDVI-derived attribute. Different letters indicate significant differences ( $P < 0.01$ ; Tukey's test). Gray bars correspond to the Eurosiberian vegetation types and white bars to the Mediterranean ones. See "Study Area" subsection for vegetation type abbreviations



semiarid vegetation types (Mediterranean semiarid scrubs and Alpha-steppes). The lowest coefficient of variation of maximum NDVI occurred in the Euro-siberian vegetation types and in the Mediterranean sclerophyllous forests. The inter-annual coefficient of variation of MIN (Fig. 6d) was significantly higher for the Alpine grasslands. Semiarid vegetation types also showed high inter-annual differences in minimum NDVI, while the rest of vegetation types showed relatively low variability. Spanish Juniper woodlands, Heathlands, Mediterranean sclerophyllous forests, and Alpine coniferous forests showed significant differences with the rest of the vegetation units for the variability (inter-annual standard deviation) in the timing of the maximum NDVI (MMAX) (Fig. 6e). In the case of the month of the minimum NDVI (MMIN), Spanish Juniper woodlands and Mediterranean coniferous and sclerophyllous forest also displayed the highest inter-annual variability, while the lowest variation occurred in Mediterranean grasslands, Dehesas, and Alpha-steppes (Fig. 6f).

#### Relationship between climatic variables and the NDVI attributes for the Iberian vegetation types

Only mean annual precipitation (MAP) showed a significant, positive relationship with NDVI-I in the multiple linear regression analysis carried out between this functional attribute and the climatic variables (Table 3). MAP explained 42% (Table 3) of the variability of the mean NDVI-I of the Iberian vegetation types ( $n = 13$ ). The analysis based on all pixels ( $n = 200$ ) showed that a lower, but significant proportion of the variance was explained by MAP (adjusted coefficient of determination  $r^2 = 0.339$ ,  $P < 0.001$ ). A logarithmic model substantially increased the proportion of the spatial variance of NDVI-I accounted by MAP (considering mean values:  $r^2 = 0.623$ ,  $n = 13$ ,  $P < 0.009$ , SE (Standard Error of the model) = 0.087; including all pixels:  $r^2 = 0.537$ ,  $n = 200$ ,  $P < 0.001$ , SE = 0.080). None of the three temperature variables considered (mean, maximum, and minimum) explained the residuals of the logarithmic relationship between MAP and NDVI-I at the Iberian scale. The Mahalanobis and Cook's distances as well as the Deleted Residual criteria showed that Alpine grasslands could be considered as an outlier in the logarithmic regression between MAP

and NDVI-I. When sites of this vegetation type were removed, the variance explained by the logarithmic model increased up to 83% ( $r^2 = 0.831$ ,  $n = 12$ ,  $P < 0.001$ , SE = 0.060; for all pixels:  $r^2 = 0.724$ ,  $n = 190$ ,  $P < 0.001$ , SE = 0.063) (Fig. 7). In the Mediterranean vegetation types, MAP linearly explained 92% of the variance in NDVI-I (Table 3, for all sites:  $r^2 = 0.703$ ,  $n = 159$ ,  $P < 0.001$ ). In the Euro-siberian vegetation types, only mean temperature (MAT) showed a significant, positive relationship with NDVI-I (Table 3; for all pixels:  $r^2 = 0.778$ ,  $n = 41$ ,  $P < 0.001$ ).

Multiple linear regressions between RREL and climatic variables only showed significant relationships when Mediterranean and Euro-siberian vegetation were analyzed separately (Table 3). For the Mediterranean vegetation types, RREL was positively related to maximum temperature (TMAX) and negatively to MAP (Table 3; with all pixels:  $r^2 = 0.577$ ,  $n = 159$ ,  $P < 0.001$ ). On the other hand, in the Euro-siberian vegetation types, RREL was negatively associated with MAT (Table 3; with all pixels it was negatively associated with TMAX:  $r^2 = 0.782$ ,  $n = 41$ ,  $P < 0.001$ ).

The inter-annual variability of the NDVI-I (CVt NDVI-I) in the Iberian vegetation types was associated with both precipitation and temperature (Table 3). The multiple regression analysis identified an inverse relationship of CVt NDVI-I with MAP and TMAX and a positive one with minimum temperature (TMIN) (Table 3; including all sites TMAX was substituted by MAT in the model:  $r^2 = 0.480$ ,  $n = 200$ ,  $P < 0.001$ ). Considering separately the mean values for the Euro-siberian and Mediterranean vegetation types, the multiple linear regressions were only significant for the latter. For Mediterranean vegetation, CVt NDVI-I was negatively associated with MAP and positively with TMIN (Table 3; for all pixels MAT also showed a negative relationship:  $r^2 = 0.689$ ,  $n = 159$ ,  $P < 0.001$ ). For the Euro-siberian vegetation, only when all pixels were considered in the multiple linear regression, CVt NDVI-I displayed a significant, negative relationship with MAT and MAP, and a positive but not significant one with TMIN ( $r^2 = 0.765$ ,  $n = 41$ ,  $P < 0.001$ ).

No significant relationship was found between the inter-annual variability of RREL (CVt RREL) and the three climatic variables for the Iberian vegetation types (Table 3). In the Mediterranean ones, a significant,

**Table 3** Multiple linear regressions carried out between the NDVI-derived attributes (descriptors of mean and inter-annual variation of productivity and seasonality) and the climatic variables for the Iberian vegetation types altogether, and for both the Mediterranean and Eurosiberian ones separately

	Iberian vegetation types <i>n</i> = 13						Eurosiberian vegetation types <i>n</i> = 5						Mediterranean vegetation types <i>n</i> = 8					
	MAP	MAT	TMAX	TMIN	MAP	MAT	TMAX	TMIN	MAP	MAT	TMAX	TMIN	MAP	MAT	TMAX	TMIN		
NDVI-I	Order & SE	1	4	2	3	0.091			1	2	3	0.015	1			0.420		
	Beta	1.186	3.743	-0.695	-2.749				4.792	-2.935	-1.061		0.963					
	<i>P</i> -value	0.004*	0.267	0.620	0.210	0.022*			0.019*	0.267	0.237	0.110	0.000			0.000*		
	Adj. <i>r</i> <sup>2</sup>	0.424	0.019	0.117	0.027	0.587			0.838 <sup>a</sup>	0.050	0.082	0.970 <sup>a</sup>	0.916 <sup>a</sup>			0.916 <sup>a</sup>		
RREL	Order & SE								1			0.147	2	1		0.129		
	Beta								-0.948				-0.499			0.629		
	<i>P</i> -value								0.014*			0.014*	0.047*			0.021*		
	Adj. <i>r</i> <sup>2</sup>								0.866 <sup>a</sup>			0.866 <sup>a</sup>	0.225			0.770		
CVt NDVI-I	Order & SE	1	2	3	3	0.039	2	1	1	3	0.002	1	3	2	0.019			
	Beta	-0.992	-1.033	0.687	0.687		-0.394	-1.684		0.613			-0.835	-0.124	0.424			
	<i>P</i> -value	0.007*	0.015*	0.035*	0.009*	0.009*	0.103	0.063		0.160	0.033*	0.002*	0.002*	0.336	0.019*	0.003*		
	Adj. <i>r</i> <sup>2</sup>	0.319	0.081	0.205	0.605	0.605	0.026	0.952 <sup>a</sup>		0.019	0.997 <sup>a</sup>	0.770	0.003	0.153	0.926 <sup>a</sup>			
CVt RREL	Order & SE								1			0.075	2	1	3	0.034		
	Beta								0.763				4.695	-2.512	-3.722			
	<i>P</i> -value								0.134			0.134	0.105	0.028*	0.119	0.008*		
	Adj. <i>r</i> <sup>2</sup>								0.443			0.443	0.021	0.801 <sup>a</sup>	0.066	0.887 <sup>a</sup>		

Blanks mean no linear relationship

NDVI-I annual mean; RREL relative range; MAP mean annual precipitation; MAT mean annual temperature; TMAX maximum temperature; TMIN minimum temperature; SE Standard Error of the model (in italics)

\* Highlights *P*-values <0.1

<sup>a</sup> Highlights adjusted *r*<sup>2</sup> > 0.8

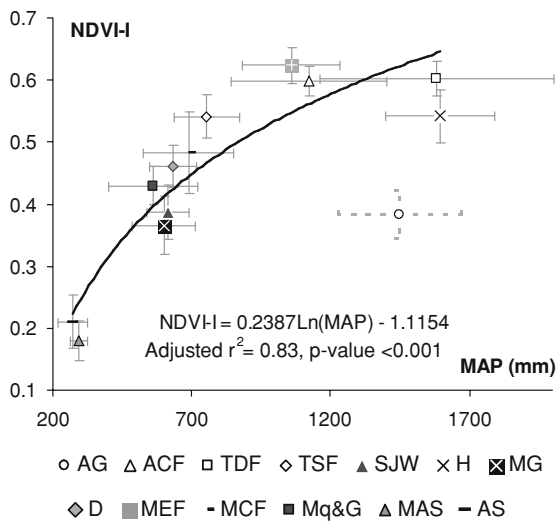


**Fig. 7** Relationship between the mean values of NDVI-I (annual mean, surrogate of productivity) and mean annual precipitation (MAP) for the Iberian vegetation types. The logarithmic model offered the best adjustment. Alpine grasslands (AG) were revealed as an outlier. *Triangles* were used for the Eurosiberian vegetation types. See “Study Area” subsection for vegetation type abbreviations

negative association was only found with TMAX. CVt RREL was also related, but not significantly, to MAT (positively) and TMIN (negatively) (Table 3). Including all Mediterranean pixels in the analysis, CVt RREL displayed significant relationships with both TMAX (negative) and MAP (positive) ( $r^2 = 0.527$ ,  $n = 159$ ,  $P < 0.001$ ). In the Eurosiberian pixels, a significant, positive relationship was found between CVt RREL and MAT ( $r^2 = 0.410$ ,  $n = 41$ ,  $P < 0.001$ ).

## Discussion

Our approach, based on a regional analysis of functional attributes of natural vegetation types, provided a description of how different attributes of ecosystem functioning change across the main environmental gradients of the Iberian Peninsula. This reference description provides baseline conditions of ecosystem functioning for the evaluation of the impact of human activities on ecosystems processes. The inter-annual variability is a critical element for this evaluation because it provides the basis for identifying anomalous behavior, such as the effect of human disturbances or extreme climatic conditions on vegetation.

The high correlation between scores in the PCA axes and the NDVI annual mean (NDVI-I) and relative range (RREL) suggests that the ecosystem functioning of the Iberian vegetation types mainly differs in terms of total production and seasonality. PCA-1 was strongly correlated with the annual mean of the NDVI, and accounted for most of the total variance in the seasonal dynamics of the NDVI (Table 2), as found in previous studies (Townshend et al. 1985; Paruelo and Lauenroth 1998; Alcaraz-Segura et al. 2006). PCA-2 was related to seasonality and phenology (as in Alcaraz-Segura et al. 2006, including non-natural land-uses). Vegetation types with high and positive scores for PCA-2 showed very high seasonality and winter minima associated with low temperatures (Fig. 3). This was the common pattern in Eurosiberian vegetation. Pixels in the negative extreme of PCA-2 also showed strong differences in NDVI among seasons, but in this case, related to the summer minima caused by the typical summer drought of the Mediterranean climates.

The representation (Fig. 8a) of NDVI-I versus RREL (the main descriptors of the NDVI dynamics from the PCA) provides, in a simple way, an overall description of the distribution of the Iberian vegetation types in the functional space defined by total production and seasonality. The separation among vegetation types in the first two PCA axes (Fig. 3) or in the NDVI-I versus RREL planes (Fig. 8a) was higher (with lower overlapping among polygons) than in the climatic plane (Fig. 8b) defined by temperature and precipitation (e.g., Whittaker 1970). The NDVI dynamics allowed us to identify a functional signature for each major vegetation type. Such functional range captures differences among vegetation units that go beyond the range of climatic factors that they experience.

Differences in light interception occurred mainly during summer and between Eurosiberian and Mediterranean vegetation types. Such differences may be related to climatic, physiological, and structural features. The Iberian vegetation differed in the seasonal distribution of the growing periods according to the timing of the different stress sources. Six patterns can be identified: (1) Unimodal NDVI seasonal dynamics with a unique and well-defined growing season centered in summer (Alpine grasslands and Temperate deciduous forests and, with lower seasonality, Temperate semideciduous forests,

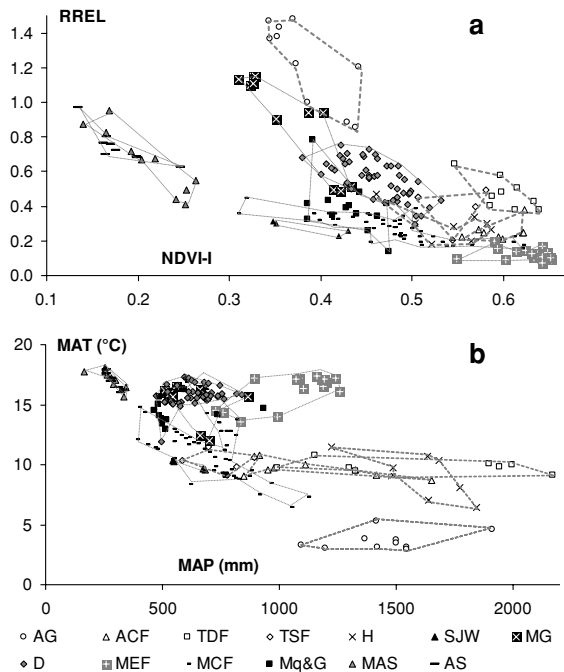


**Fig. 8** **a** Spatial heterogeneity and functional space of the Iberian vegetation types in terms of NDVI-I (an estimator of productivity) and RREL (a surrogate of seasonality). **b** Climatic characterization in terms of mean annual temperature (MAT) and precipitation (MAP) of the same pixels. *Dashed lines* correspond to the Eurosiberian vegetation types and *continuous lines* to the Mediterranean ones. See “Study Area” subsection for vegetation type abbreviations

Heathlands, and Alpine coniferous forests). (2) High NDVI throughout the year, with relative spring and autumn maxima and winter and summer minima (Mediterranean sclerophyllous forests; similar dynamics but with lower NDVI was observed in Mediterranean coniferous forests). (3) Bimodal NDVI profile with two clear growing periods with maxima in late-autumn and late-spring as well as minima caused by both severe winters and summers (Spanish Juniper woodlands). (4) NDVI seasonal profile with a growing season with late-autumn maxima and summer minima (Maquis and garrigues, i.e., seasonal heteromorphic evergreen chamaephytic formations with slight toleration to cold and drought stresses). (5) Low NDVI values throughout the year and a slight growing season centered in winter (Mediterranean summer-deciduous semiarid scrublands and Alpha-steppes). (6) NDVI profile with a strong and pronounced summer minima (Dehesas and especially Mediterranean grasslands).

Vegetation structure and climatic conditions explained the differences in inter-annual variability

of the NDVI dynamics among the Iberian vegetation types. The inter-annual variability of the Mediterranean climate limits the regularity and duration of the favorable periods for vegetation growing in this region, where, for instance, variability of rainfall is twice that one observed in the Eurosiberian part (Rodó and Comín 2001). As expected, Mediterranean vegetation types presented in general higher inter-annual variability of the NDVI dynamics. Aside from the effect of climate, the plant functional type composition may account for the high variability of Mediterranean ecosystems. Annual grasses and forbs are an important component of them, which generates a low buffer capacity (lower inertia) that makes the system more dependent on climate variability (Wiegand et al. 2004). In fact, the lower NDVI-I inter-annual variability of Dehesas compared to Mediterranean grasslands could be related to the presence of sclerophyllous trees in the former. Inter-annual variability for MAX in the Eurosiberian vegetation (in summer) was low due the reliability of precipitation compared to Mediterranean areas (Orshan 1989). In the case of Alpine grasslands, the high inter-annual variability observed in the MIN (winter) could be associated with year to year changes in snow cover between November and April (del Barrio et al. 1990).

As in previous studies, we found a logarithmic relationship between precipitation and NDVI-I (e.g., Box et al. 1989; Paruelo and Lauenroth 1995). The response of NDVI-I to MAP in the Mediterranean reveals the restriction of water availability in these ecosystems (Di Castri et al. 1981; Blondel and Aronson 1999). The logarithmic model found may be explained by the restriction that low temperatures and vegetation structure impose to plant growth, particularly in some vegetation types of the Eurosiberian Region (Chabot and Hicks 1982). This is particularly evident for Alpine grasslands, where high altitude (low temperatures and snow cover), low cover, and herbs dominance impose a structural constraint to light absorption during the growing season, despite water availability. Besides, most annual precipitation falls as snow when vegetation is dormant and, after melting, it leaves the system as streamflow. Heathlands have the same limiting factors but under less severe constraints. In fact, mean temperature was the main significant constraint to NDVI-I in the Eurosiberian vegetation. Hence, while water imposes a limitation in the Mediterranean

vegetation types, temperature constrains productivity in the Eurosiberian ones.

The climatic controls of seasonality (RREL) varied between regions. In the Mediterranean, the summer maximum temperatures showed the strongest relationship with seasonality, but the influence of temperature was partially reduced when precipitation was high. In contrast, in the Eurosiberian vegetation types, mean temperature caused the opposite effect on the RREL: seasonality was lower under warmer conditions. Differences in NDVI among seasons are caused by low winter temperatures in the Eurosiberian vegetation types and by summer drought (higher maximum temperatures and lower precipitations) in the Mediterranean ones.

Inter-annual variability of the NDVI-I decreased as climatic conditions (precipitation and extreme temperatures) became less limiting for plant growth. In general, variability in precipitation decreases from xeric to mesic conditions (e.g., Montero de Burgos and González-Rebollar 1983; Rodó and Comín 2001). In fact, the highest inter-annual differences in NDVI-I were found in the semiarid vegetation (Semiarid scrublands and Alpha-steppes), which is known to undergo significant inter-annual fluctuations in precipitation (Lázaro et al. 2001). In contrast, inter-annual differences in seasonality (CVt RREL) in the Mediterranean pixels tended to be higher in mesic sites (higher precipitation and lower maximum temperatures), as well as in the Eurosiberian ones, where they increased with warmer conditions. In such mesic conditions, seasonality is very low, making it prone to suffer high inter-annual differences as a result of climate variability.

## Conclusions

The NDVI seasonal dynamics was able to characterize the spatio-temporal heterogeneity of ecosystem functioning in the largest remaining patches of the Iberian vegetation types. By describing the inter-annual variability, such characterization not only evaluates the buffer capacity of different vegetation structures to climate variability, but also provides a reference of ecosystem functioning to evaluate the effects of global environmental changes. For instance, it would allow the identification of extreme periods and deviations from recorded values (Garbulsky and Paruelo 2004;

Paruelo et al. 2005). This information has several applications in management of natural areas, such as how many growing periods there exist in a year, when do they start, peak, and end, or how much biomass would be available for heterotrophes in different seasons (see Pettorelli et al. 2005).

The functional signatures of each vegetation type identified from the NDVI dynamics capture differences in space and time among vegetation units that integrate the range of environmental factors that they experience. The Iberian vegetation types mainly differed in terms of total production and seasonality. These differences were largely related to the contrasting patterns of precipitation and temperature of the Mediterranean and Eurosiberian regions. Such patterns also conditioned the inter-annual variability of the functional attributes. The baseline descriptions that we provide here have, in our opinion, a particular advantage to be incorporated in monitoring programs: they are based on a common approach to characterize vegetation functioning from remotely sensed images. Though the present approach had to be based on coarse spatial resolution imagery to gain enough number of years that captured the long-term variability (e.g., both dry and wet periods), it will favor from higher resolution sensors as soon as longer data records become available (e.g., MODIS is available since year 2000). In addition, the higher resolution and quality assessment of current sensors allows for a lower influence of clouds and aerosols. This is not a big concern for the Iberian Peninsula, but it may influence the analysis in areas where clouds and smoke from fires are a considerable factor (e.g., the tropics).

**Acknowledgments** The authors are grateful to the editor and two anonymous referees for their suggestions that improved the manuscript. P. Escribano, P. Durante, and M. Torres helped compositing the Spanish Forest Map. Financial support was given by Postdoctoral program of Ministerio de Educación y Ciencia, FEDER funds, Junta de Andalucía (projects RNM1288 and RNM1280), Organismo Autónomo de Parques Nacionales (project 066/2007), Ecología de Zonas Áridas Research Group, University of Almería, Proyecto Estratégico of the University of Buenos Aires, CONICET, and FONCYT. Satellite data were provided by the EOS-DAAC at Goddard Space Flight Center (NASA-NOAA). CORINE land-cover database was provided by the EIONET—European Environmental Agency.

## Appendix

See Table 4

**Table 4** Mahalanobis distances (lower left side) and *F*-values for the distances (upper right side) between the centroids of each vegetation type group

	AG	ACF	TDF	TSF	H	SJW	MG	D	MEF	MCF	Mq&G	MAS	AS
AG		137	35	22	38	31	116	162	91	105	85	57	53
ACF	45		15	3	5	8	35	32	6	8	12	32	33
TDF	106	48		6	81	100	200	143	68	85	118	145	158
TSF	101	13	28		24	36	115	80	37	30	47	81	90
H	122	16	24	5		7	27	61	14	13	14	28	96
SJW	173	48	17	5	40		10	51	12	6	5	10	60
MG	312	100	70	26	83	57		12	34	52	37	64	72
D	273	59	77	23	29	11	8		27	51	15	39	77
MEF	212	16	27	9	38	63	74	32		19	30	103	118
MCF	176	16	46	9	27	28	34	27	16		6	54	64
Mq&G	210	33	44	11	40	25	16	20	15	4		19	55
MAS	161	96	48	18	89	54	24	66	44	32	47		1
AS	160	107	50	19	28	10	25	41	47	34	21	0	

All *F*-values are significant ( $P < 0.001$ ) except for AS versus MAS

See “Study Area” subsection for vegetation type abbreviations

## References

- Alcaraz-Segura D, Paruelo JM, Cabello J (2006) Identification of current ecosystem functional types in the Iberian Peninsula. *Glob Ecol Biogeogr* 15:200–212. doi:[10.1111/j.1466-822X.2006.00215.x](https://doi.org/10.1111/j.1466-822X.2006.00215.x)
- Alcaraz-Segura D, Cabello J, Paruelo JM, Delibes M (2008a) Use of descriptors of ecosystem functioning for monitoring a National Park network: a remote sensing approach. *Environ Manage*. doi:[10.1007/s00267-008-9154-y](https://doi.org/10.1007/s00267-008-9154-y)
- Alcaraz-Segura D, Cabello J, Paruelo JM, Delibes M (2008b) Trends in the surface vegetation dynamics of the National Parks of Spain as observed by satellite sensors. *Appl Veg Sci* 11:431–440. doi:[10.3170/2008-7-18522](https://doi.org/10.3170/2008-7-18522)
- Baldi G, Noretto MD, Aragón R, Aversa F, Paruelo JM, Jobbágy EG (2008) Long-term satellite NDVI data sets: evaluating their ability to detect ecosystem functional changes in South America. *Sensors* 8:5397–5425. doi:[10.3390/s8095397](https://doi.org/10.3390/s8095397)
- Blondel J, Aronson J (1999) *Biology and wildlife of the Mediterranean region*. Oxford University Press, New York
- Box EO, Holben BN, Kalb V (1989) Accuracy of the AVHRR vegetation index as a predictor of biomass, primary productivity and net CO<sub>2</sub> flux. *Vegetatio* 80:71–89. doi:[10.1007/BF00048034](https://doi.org/10.1007/BF00048034)
- Chabot BF, Hicks DJ (1982) The ecology of leaf life spans. *Annu Rev Ecol Syst* 13:229–259. doi:[10.1146/annurev.es.13.110182.001305](https://doi.org/10.1146/annurev.es.13.110182.001305)
- Costa M, Morla C, Sainz H (2005) *Los bosques ibéricos: una interpretación geobotánica*. Planeta, Barcelona
- Daily GC (1997) *Nature's services: societal dependence on natural ecosystems*. Part III. Services supplied by major biomes. Island Press, Washington, DC
- de Beurs K, Henebry G (2007) War, drought, and phenology: changes in the land surface phenology of Afghanistan since 1982, vol 4. In: *IEEE international conference on geoscience and remote sensing symposium, 2006 (IGARSS 2006)*, pp 2432–2435
- de Castro M, Martín-Vide J, Alonso S (2005) El clima de España: pasado, presente y escenarios de clima para el siglo XXI. In: *Moreno-Rodríguez JM (ed) Evaluación preliminar de los impactos en España por efecto del cambio climático*. Ministerio de Medio Ambiente, Madrid, pp 1–64
- del Barrio G, Creus J, Puigdefábregas J (1990) Thermal seasonality of the high mountain belts of the Pyrenees. *Mt Res Dev* 10:227–233. doi:[10.2307/3673602](https://doi.org/10.2307/3673602)
- Di Castri F, Goodall DW, Specht RL (1981) *Mediterranean-type shrublands*. Elsevier, Amsterdam
- EEA (European Environmental Agency) (2000) *The 1990 CORINE land cover database (CLC90—100 m grid—version 12, 2000)*
- EEA (European Environmental Agency) (2007) *The 1990–2000 CORINE land cover change database (CLC90–CLC00—100 m grid—version 9, 2007)*
- Fazey I, Fischer J, Lindenmayer DB (2005) What do conservation biologists publish? *Biol Conserv* 124:63–73. doi:[10.1016/j.biocon.2005.01.013](https://doi.org/10.1016/j.biocon.2005.01.013)
- Garbulsky MF, Paruelo JM (2004) Remote sensing of protected areas to derive baseline vegetation functioning characteristics. *J Veg Sci* 15:711–720. doi:[10.1658/1100-9233\(2004\)015\[0711:RSOPAT\]2.0.CO;2](https://doi.org/10.1658/1100-9233(2004)015[0711:RSOPAT]2.0.CO;2)
- Hicke JA, Asner GP, Randerson JT, Tucker C, Los S, Birdsey R, Jenkins JC, Field C (2002) Trends in North American net primary productivity derived from satellite observations, 1982–1998. *Global Biogeochem Cycles* 16(2). doi:[10.1029-2001GB001550](https://doi.org/10.1029-2001GB001550)

- Hoare D, Frost P (2004) Phenological description of natural vegetation in southern Africa using remotely-sensed vegetation data. *Appl Veg Sci* 7:19–28. doi:[10.1658/1402-2001\(2004\)007\[0019:PDONVI\]2.0.CO;2](https://doi.org/10.1658/1402-2001(2004)007[0019:PDONVI]2.0.CO;2)
- Holben BN (1986) Characteristics of maximum-value composite images for temporal AVHRR data. *Int J Remote Sens* 7:1417–1434. doi:[10.1080/01431168608948945](https://doi.org/10.1080/01431168608948945)
- James ME, Kalluri SNV (1994) The Pathfinder AVHRR Land data set: an improved coarse resolution data set for terrestrial monitoring. *Int J Remote Sens* 15:3347–3363. doi:[10.1080/01431169408954335](https://doi.org/10.1080/01431169408954335)
- Julien Y, Sobrino JA, Verhoef W (2006) Changes in land surface temperatures and NDVI values over Europe between 1982 and 1999. *Remote Sens Environ* 103:43–55. doi:[10.1016/j.rse.2006.03.011](https://doi.org/10.1016/j.rse.2006.03.011)
- Lázaro R, Rodrigo FS, Gutiérrez L, Domingo F, Puigdefábregas J (2001) Analysis of a 30-year rainfall record (1967–1997) in semi-arid SE Spain for implications on vegetation. *J Arid Environ* 48:373–395. doi:[10.1006/jare.2000.0755](https://doi.org/10.1006/jare.2000.0755)
- Lieth H (1974) *Phenology and seasonality*. Springer-Verlag, Berlin
- Lloyd D (1990) A phenological classification of terrestrial vegetation cover using shortwave vegetation index imagery. *Int J Remote Sens* 11:2269–2279. doi:[10.1080/01431169008955174](https://doi.org/10.1080/01431169008955174)
- Lobell DB, Hicke JA, Asner GP, Field CB, Tucker CJ, Los SO (2002) Satellite estimates of productivity and light use efficiency in United States agriculture, 1982–1998. *Glob Chang Biol* 8:722–735. doi:[10.1046/j.1365-2486.2002.00503.x](https://doi.org/10.1046/j.1365-2486.2002.00503.x)
- McNaughton SJ, Oesterheld M, Frank DA, Williams KJ (1989) Ecosystem-level patterns of primary productivity and herbivory in terrestrial habitats. *Nature* 341:142–144. doi:[10.1038/341142a0](https://doi.org/10.1038/341142a0)
- Milchunas DG, Lauenroth WK (1995) Inertia in plant community structure: state changes after cessation of nutrient enrichment stress. *Ecol Appl* 5:1195–2005. doi:[10.2307/1942035](https://doi.org/10.2307/1942035)
- Mitrakas K (1980) A theory for Mediterranean plant life. *Acta Oecol* 1:245–252
- Monteith JL (1972) Solar radiation and productivity in tropical ecosystems. *J Appl Ecol* 9:747–766. doi:[10.2307/2401901](https://doi.org/10.2307/2401901)
- Montero de Burgos JL, González-Rebollar JL (1983) Diagramas bioclimáticos. Instituto para la Conservación de la Naturaleza, Madrid
- Mooney HA, Kummerow J, Johnons W, Parsons DJ, Keeley S, Hoffmann A, Hays RI, Giliberto J, Chu C (1977) The producers-their resources and adaptive responses. Convergent evolution in Chile and California. Mediterranean climate ecosystems. Dowden, Hutchinson & Ross, Stroudsburg, pp 85–143
- Mueller Dombos D, Ellenberg H (1974) *Aims and methods of vegetation ecology*. Wiley, New York
- Myneni RB, Williams DL (1994) On the relationship between fAPAR and NDVI. *Remote Sens Environ* 49:200–211. doi:[10.1016/0034-4257\(94\)90016-7](https://doi.org/10.1016/0034-4257(94)90016-7)
- Nemani RR, Keeling CD, Hashimoto H, Jolly WM, Piper SC, Tucker CJ, Myneni RB, Running SW (2003) Climate-driven increases in global terrestrial net primary production from 1982 to 1999. *Science* 300:1560–1563. doi:[10.1126/science.1082750](https://doi.org/10.1126/science.1082750)
- Orshan G (1989) *Plant pheno-morphological studies in Mediterranean type ecosystems*. Kluwer, Dordrecht
- Paruelo JM, Lauenroth WK (1995) Regional patterns of Normalized Difference Vegetation Index in North American shrublands and grasslands. *Ecology* 76:1888–1898. doi:[10.2307/1940721](https://doi.org/10.2307/1940721)
- Paruelo JM, Lauenroth WK (1998) Interannual variability of NDVI and its relationship to climate for North American shrublands and grasslands. *J Biogeogr* 25:721–733. doi:[10.1046/j.1365-2699.1998.2540721.x](https://doi.org/10.1046/j.1365-2699.1998.2540721.x)
- Paruelo JM, Epstein HE, Lauenroth WK, Burke IC (1997) ANPP estimates from NDVI for the Central Grassland Region of the United States. *Ecology* 78:953–958
- Paruelo JM, Jobbágy EG, Sala OE (2001) Current distribution of ecosystem functional types in temperate South America. *Ecosystems* 4:683–698. doi:[10.1007/s10021-001-0037-9](https://doi.org/10.1007/s10021-001-0037-9)
- Paruelo JM, Garbulsky MF, Guerschman JP, Jobbágy EG (2004) Two decades of Normalized Difference Vegetation Index changes in South America: identifying the imprint of global change. *Int J Remote Sens* 25:2793–2806. doi:[10.1080/01431160310001619526](https://doi.org/10.1080/01431160310001619526)
- Paruelo JM, Piñeiro G, Oyonarte C, Alcaraz-Segura D, Cabello J, Escribano P (2005) Temporal and spatial patterns of ecosystem functioning in protected arid areas of South-eastern Spain. *Appl Veg Sci* 8:93–102. doi:[10.1658/1402-2001\(2005\)008\[0093:TASPOE\]2.0.CO;2](https://doi.org/10.1658/1402-2001(2005)008[0093:TASPOE]2.0.CO;2)
- Pettorelli N, Vik JO, Myrseterud A, Gaillard JM, Tucker CJ, Stenseth NC (2005) Using the satellite-derived NDVI to assess ecological responses to environmental change. *Trends Ecol Evol* 20:503–510. doi:[10.1016/j.tree.2005.05.011](https://doi.org/10.1016/j.tree.2005.05.011)
- Rathcke B, Lacey EP (1985) Phenological patterns of terrestrial plants. *Annu Rev Ecol Syst* 16:179–214. doi:[10.1146/annurev.es.16.110185.001143](https://doi.org/10.1146/annurev.es.16.110185.001143)
- Rivas-Martínez S (1987) Mapa de series de vegetación de España 1:400000 y Memoria. ICONA, Madrid
- Rodó X, Comín F (2001) Fluctuaciones del clima mediterráneo: conexiones globales y consecuencias regionales. In: Zamora R, Pugnaire FI (eds) *Aspectos funcionales de los ecosistemas mediterráneos*. CSIC-AEET, Granada, pp 1–36
- Ruiz de la Torre J (1999) Mapa Forestal de España 1:200.000 - MFE200, Organismo Autónomo de Parques Nacionales. Ministerio de Medio Ambiente, Madrid
- Sánchez-Palomares O, Sánchez-Serrano F, Carretero-Carrero MP (1999) Modelos y cartografía de estimaciones climáticas termoplumiométricas para la España peninsular. INIA, Madrid
- Sarkar C, Bhattacharya BK, Gadgil A, Mallick K, Patel NK, Parihar JS (2008) Estimation of relative evapotranspiration from NOAA PAL to derive growth characteristics in India. *Int J Remote Sens* 29:3271–3293. doi:[10.1080/01431160701442112](https://doi.org/10.1080/01431160701442112)
- Sellers PJ, Berry JA, Collatz GJ, Field CB, Hall FG (1992) Canopy reflectance, photosynthesis, and transpiration. III. A reanalysis using improved leaf models and a new canopy integration scheme. *Remote Sens Environ* 42:187–216. doi:[10.1016/0034-4257\(92\)90102-P](https://doi.org/10.1016/0034-4257(92)90102-P)
- Sellers PJ, Randall DA, Collatz GJ, Berry JA, Field CB, Dazlich DA, Zhang C, Collole GD, Bounoua L (1996) A revised Land Surface parameterization (SiB2) for



- atmospheric GCMs. Part I: model formulation. *J Clim* 9:676–705. doi:10.1175/1520-0442(1996)009<0676:ARLSPF>2.0.CO;2
- Sobrino JA, Julien Y, Morales L (2006) Multitemporal analysis of PAL images for the study of land cover dynamics in South America. *Glob Planet Chang* 51:172–180. doi:10.1016/j.gloplacha.2006.01.006
- Stephenson NL (1990) Climatic control of vegetation distribution: the role of the water balance. *Am Nat* 135:649–670. doi:10.1086/285067
- Stevenson AC, Harrison RJ (1992) Ancient forests in Spain: a model for land-use and dry forest management in southwest Spain from 4000 BC to 1900 AD. *Proc Prehist Soc* 58:227–247
- Townshend JRG, Goff TE, Tucker CJ (1985) Multitemporal dimensionality of images of Normalized Difference Vegetation Index at continental scales. *IEEE Trans Geosci Remote Sens* 23:888–895. doi:10.1109/TGRS.1985.289474
- Tucker CJ, Sellers PJ (1986) Satellite remote-sensing of primary production. *Int J Remote Sens* 7:1395–1416. doi:10.1080/01431168608948944
- Tucker CJ, Townshend JR, Goff TE (1985) African land-cover classification using satellite data. *Science* 227:369–375. doi:10.1126/science.227.4685.369
- Valentini R, Baldocchi DD, Tenhunen JD (1999) Ecological controls on land-surface atmospheric interactions. In: Tenhunen JD, Kabat P (eds) *Integrating hydrology, ecosystem dynamics and biogeochemistry in complex landscapes*. Wiley, Berlin, pp 105–116
- Valladares F, Camarero JJ, Pulido F, Gil-Pelegrín E (2004) El bosque mediterráneo, un sistema humanizado y dinámico. In: Valladares F (ed) *Ecología del bosque mediterráneo en un mundo cambiante*. Organismo Autónomo de Parques Nacionales. Ministerio de Medio Ambiente, Madrid, pp 13–26
- Virginia RA, Wall DH (2001) Principles of ecosystem function. In: Levin SA (ed) *Encyclopedia of biodiversity*. Academic Press, San Diego, pp 345–352
- Vitousek PM, Mooney HA, Lubchenco J, Melillo JM (1997) Human domination of Earth's ecosystems. *Science* 277:494–499. doi:10.1126/science.277.5325.494
- Whittaker RH (1970) *Communities and ecosystems*. MacMillan, New York
- Wiegand T, Snyman HA, Kellner K, Paruelo JM (2004) Do grasslands have a memory: modeling phytomass production of a semiarid South African grassland. *Ecosystems* 7:243–258. doi:10.1007/s10021-003-0235-8
- Wolters V, Silver WL, Bignell DE, Coleman DC, Lavelle P, van der Putten W, de Ruiter P, Rusek J, Wall DH, Wardle DA, Brussaard L, Dangerfield JM, Brown VK, Giller K, Hooper DU, Sala OE, Tiedje J, van Veen JA (2000) Effects of global changes on above and belowground biodiversity in terrestrial ecosystems: implications for ecosystem functioning. *Bioscience* 50:1089–1098. doi:10.1641/0006-3568(2000)050[1089:EOGCOA]2.0.CO;2
- Xiao J, Moody A (2004) Photosynthetic activity of US biomes: responses to the spatial variability and seasonality of precipitation and temperature. *Glob Chang Biol* 10:437–451. doi:10.1111/j.1365-2486.2004.00745.x